

Angular correlations in $B\bar{B}$ pair production at the LHC in the parton Reggeization approach

Anton Karpishkov^{1,*}, Maxim Nefedov^{1,**}, and Vladimir Saleev^{1,***}

¹Samara National Research University - 34, Moskovskoe Shosse, Samara, 443086, Russia

Abstract. We calculate angular correlation spectra between beauty (B) and anti-beauty (\bar{B}) mesons in proton-proton collisions in the leading order approximation of the parton Reggeization approach consistently merged with the next-to-leading order corrections from the emission of additional hard gluon (NLO* approximation). To describe b -quark hadronization we use the universal scale-depended parton-to-meson fragmentation functions extracted from the combined e^+e^- annihilation data. The Kimber-Martin-Ryskin model for the unintegrated parton distribution functions in a proton is implied. We have obtained good agreement between our predictions and data from the CMS Collaboration at the energy $\sqrt{S} = 7$ TeV for $B\bar{B}$ angular correlations within uncertainties and without free parameters.

1 Introduction

Production of bottom-flavored mesons (B) and b -quarks in the high energy pp -collisions is the object of an intensive experimental study at the CERN LHC. Physics of beauty quarks is very interesting for test of higher-order radiative corrections in Quantum Chromodynamics (QCD), for search of new exotic bound states of heavy quarks and for precise study of parameters of the Standard Model in the flavor sector. Measurements of $b\bar{b}$ angular and momentum correlations provide a test of dynamics of hard interactions, which is sensitive to the next-to-leading order (NLO) corrections of QCD. There are two ways to study this $b\bar{b}$ correlations. The first one is based on a reconstruction of pairs of b -jets [1, 2], in the second case we get an information on dynamics of hard production of $b\bar{b}$ -pair using data on $B\bar{B}$ -pair production. In turn, long-lived B -mesons are reconstructed via their semileptonic decays. One advantage of this method is the unique capability to detect $B\bar{B}$ -pairs even at small opening angles, in which case the decay products of the B hadrons tend to be merged into a single jet and the standard b -jet tagging techniques are not applicable [3]. The conventional formalism of the Collinear Parton Model (CPM) is most suitable for calculation of single-scale variables, such as inclusive production cross section, transverse momentum (p_T) or rapidity spectra of B -mesons. Correlation spectra, such as the spectrum of azimuthal angle difference between B and \bar{B} transverse momenta and their rapidity differences spectrum are multi-scale observables. To describe these multi-scale quantities in perturbative QCD one should take into account significant radiative corrections

*e-mail: karpishkov@ssau.ru

**e-mail: nefedovma@gmail.com

***e-mail: saleev@samsu.ru

from the emission of hard partons with large transverse momentum. The aim of our paper is to describe $B\bar{B}$ angular correlation spectra in the Parton Reggeization Approach (PRA) of QCD, as it has been done early for dijets [4], $b\bar{b}$ -jets [5, 6], prompt photon pairs [7], $D\bar{D}$ and DD pairs [8, 9]. The novelty of our present results is the merging of Leading-Order (LO) PRA contribution and real NLO* correction from the emission of additional hard gluon.

2 Basic formalism

The PRA is gauge-invariant scheme of high-energy QCD calculations which extends the CPM for description of hard multi-scale processes at the high-energy regime, when we deal with the processes in the multi-Regge kinematics (MRK). In the MRK, energy of collision (\sqrt{S}) is sufficiently larger than transverse momenta of final particles ($\sqrt{S} \gg |\mathbf{k}_{Ti}|$) and invariant masses of their pairs ($M_{ij} = \sqrt{(k_i + k_j)^2}$). The main ingredient of the PRA are the high-energy or k_T -factorization of unintegrated parton distribution functions (unPDFs) and gauge-invariant partonic cross sections with *off-shell* partons in the initial state, where these off-shell partons are considered as Reggeized gluons (R) and Reggeized quarks (Q).

The following LO parton subprocesses are relevant for our study of $B\bar{B}$ -pair production in the PRA [10]:

$$R + R \rightarrow b + \bar{b}, \quad (1)$$

$$Q + \bar{Q} \rightarrow b + \bar{b}. \quad (2)$$

Here, we explore the main mechanisms of B -meson production via b -quark fragmentation into B -meson. At high energy and moderate transverse momenta of B -mesons, the contribution of the subprocess of quark-antiquark annihilation (2) is negligible in comparison to the gluon-gluon fusion contribution [5] and we will consider contribution of subprocess (1) only. Taking into account the experimental conditions for $B\bar{B}$ -pair production data measured by the CMS Collaboration [3], which we study, we should add contribution of NLO subprocess

$$R + R \rightarrow b + \bar{b} + g, \quad (3)$$

which generates events with leading jet originating from gluon but not from final b or \bar{b} quarks, see the discussion in the Sec. 5 below.

The general factorization formula for the cross-section in PRA reads:

$$\begin{aligned} d\sigma^{PRA}(pp \rightarrow b\bar{b} + X) &= \int \frac{dx_1}{x_1} \int \frac{d^2\mathbf{q}_{1T}}{\pi} \int \frac{dx_2}{x_2} \int \frac{d^2\mathbf{q}_{2T}}{\pi} \Phi_g(x_1, t_1, \mu^2) \times \\ &\times \Phi_g(x_2, t_2, \mu^2) \frac{|\mathcal{A}_{PRA}|^2}{2S x_1 x_2} d\Phi(k_3, k_4), \end{aligned} \quad (4)$$

where $q_{1,2}^\mu = x_{1,2}P_{1,2}^\mu + q_{1,2T}^\mu$, $t_{1,2} = -q_{1,2T}^2 = \mathbf{q}_{1,2T}^2$, $P_{1,2}^\mu$ are the four-momenta of initial-state protons, $(P_1 + P_2)^2 = S$ and $|\mathcal{A}_{PRA}|^2$ is the modulus squared of the matrix element of the corresponding PRA subprocess, which is discussed in more detail in the Sec. 3. The unintegrated gluon PDF, first introduced by Kimber, Martin and Ryskin (KMR) [11] is defined as

$$\Phi_g(x, t, \mu^2) = T_g(t, \mu^2) \frac{\alpha_s(t)}{2\pi \cdot t} \int_x^{1-\Delta} dz P_{gg}(z) \frac{x}{z} f_g\left(\frac{x}{z}, t\right), \quad (5)$$

where $\Delta(t, \mu^2) = \frac{\sqrt{t}}{\mu + \sqrt{t}}$ and the Sudakov form factor is equal to

$$T_g(t, \mu^2) = \exp \left[- \int_t^{\mu^2} \frac{\alpha_s(t')}{2\pi} \frac{dt'}{t'} \int_0^{1-\Delta(t', \mu^2)} dz' P_{gg}(z') \right].$$

The unintegrated PDF, defined by Eq. (5) approximately satisfies the normalization condition,

$$\int_0^{\mu^2} dt \Phi_g(x, t, \mu^2) = x f_g(x, \mu^2). \quad (6)$$

The relation between MRK limit of QCD scattering amplitudes and KMR unPDF is explained, and the derivation of factorization formula (4) is presented in the Ref. [12]. In a stage of numerical calculation we use the LO PDFs from the MSTW-2008 set [13] proton PDFs as collinear input.

3 Reggeized amplitudes

To obtain Reggeized amplitudes of the subprocesses (1) and (3) we exploit our in-house implementation of the Feynman rules of the Lipatov's Effective Theory of Reggeized gluons and Reggeized quarks [14, 15] as a model file for the popular automatic Feynman amplitude generator FeynArts [16]. This model file can be used to generate $2 \rightarrow 2$ and $2 \rightarrow 3$ tree-level scattering amplitudes with Reggeized quarks and Reggeized gluons in the initial state and with Yang-Mills gluons, quarks and photons in the final state. This instrument has been developed as a continuation of the work done in the Ref. [17] and will be publicly released soon, under the acronym ReggeQCD. The generated amplitudes can be further processed using FeynCalc [18] or FormCalc [19] programs.

The generated sets of Feynman diagrams for subprocesses (1) and (3) are shown in Fig. 1 and Fig. 2, correspondingly. The exact analytical formula for Reggeized amplitude $\mathcal{A}_{PRA}(RR \rightarrow b\bar{b})$ as well as its squared modulus $|\mathcal{A}_{PRA}(RR \rightarrow b\bar{b})|^2$ has been obtained earlier, see the Appendix of Ref. [4]. The squared amplitude $|\mathcal{A}_{PRA}(RR \rightarrow b\bar{b}g)|^2$ is too large for the analytical presentation in the paper. The FORTRAN code for this squared amplitude can be obtained by the request from authors.

We have checked the gauge invariance of the obtained results w. r. t. the choice of the gauge for external gluon legs and internal gluon propagators. Also it has been verified, that in the collinear limit $\mathbf{q}_{(1,2)T} \rightarrow 0$, squared amplitudes (1) and (3) transform to the squared amplitudes of the corresponding parton subprocesses in the CPM after averaging over the azimuthal angles. Additionally, we have compared our results for the both squared amplitudes numerically with the results obtained from the Monte-Carlo generator Katie [20], which is based on the recently suggested scheme to obtain gauge-invariant matrix elements in the k_T -factorization by exploiting the spinor-helicity representation and recursion relations for the tree-level amplitudes [21, 22].

4 Cross sections

The hadronic cross section of subprocess (1) in the PRA can be written as follows:

$$\begin{aligned} \frac{d\sigma(pp \rightarrow b(k_1)\bar{b}(k_2) + X)}{dy_1 dy_2 dk_{1T} dk_{2T}} &= \frac{k_{1T} k_{2T}}{16\pi^3} \int d\phi_1 \int d\Delta\phi \int dt_1 \times \\ &\times \Phi_g(x_1, t_1, \mu^2) \Phi_g(x_2, t_2, \mu^2) \frac{|\mathcal{A}_{PRA}(RR \rightarrow b\bar{b})|^2}{(x_1 x_2 S)^2}, \end{aligned} \quad (7)$$

where $\Delta\phi$ is the azimuthal angle between \mathbf{k}_{1T} and \mathbf{k}_{2T} , and $k_{Ti} = |\mathbf{k}_{Ti}|$ in the Eqns. 7 and 8.

The $2 \rightarrow 3$ differential cross section for subprocess (3) includes additional integration on phase space of final gluon $g(k_3)$ relatively $2 \rightarrow 2$ cross section (7) and reads

$$\begin{aligned} \frac{d\sigma(pp \rightarrow b(k_1)\bar{b}(k_2)g(k_3) + X)}{dy_1 dy_2 dk_{1T} dk_{2T}} &= \frac{k_{1T} k_{2T}}{(2\pi)^6} \int dy_3 \int d\phi_1 \int d\phi_2 \int dk_{3T} \times \\ &\times \int d\Delta\phi \int dt_1 \int dt_2 \Phi_g(x_1, t_1, \mu^2) \Phi_g(x_2, t_2, \mu^2) \frac{|\mathcal{A}_{PRA}(RR \rightarrow b\bar{b}g)|^2}{8(x_1 x_2 S)^2}. \end{aligned} \quad (8)$$

To describe the hadronization stage we use the fragmentation approach. The transition from the produced $b(\bar{b})$ -quark to the $B(\bar{B})$ meson is described by the corresponding fragmentation function (FF) $D_{b,g \rightarrow B}(z, \mu^2)$. According the factorization theorem of the fragmentation model, the master formula for the $B\bar{B}$ -pair production via subprocess (1) reads:

$$\begin{aligned} \frac{d\sigma(pp \rightarrow B\bar{B} + X)}{dp_{BT} dy_B dp_{\bar{B}T} dy_{\bar{B}}} &= \int_0^1 \frac{dz_1}{z_1} \int_0^1 \frac{dz_2}{z_2} D_{b \rightarrow B}(z_1, \mu^2) D_{\bar{b} \rightarrow \bar{B}}(z_2, \mu^2) \times \\ &\times \frac{d\sigma(pp \rightarrow b(k_1) + \bar{b}(k_2) + X)}{dk_{1T} dy_1 dk_{2T} dy_2}, \end{aligned} \quad (9)$$

where $D_{b \rightarrow B}(z_1, \mu^2) = D_{\bar{b} \rightarrow \bar{B}}(z_2, \mu^2)$ are the FFs for the transitions of $b(\bar{b})$ -quark into $B(\bar{B})$ meson with momentum fraction $z_1(z_2)$ at the scale μ^2 , $p_B^\mu = z_1 k_1^\mu$, and $p_{\bar{B}}^\mu = z_2 k_2^\mu$.

In our calculations we use the LO FFs from Ref. [23], where the fit of non-perturbative $b(\bar{b})$ and gluon FF's to data for the $B(\bar{B})$ production from the ALEPH [24] and OPAL [25] Collaborations at the CERN LEP1 collider has been performed. These data were taken at the energy of Z -boson peak, that strongly suppresses the finite- m_b effects which are of relative order m_b^2/m_Z^2 , giving the internal consistency of resulting FFs with the zero-mass scheme [26] which we keep throughout our analysis. These FFs satisfy two desirable properties: at first, their scaling violations are ruled by DGLAP evolution equations [27]; at second, they are universal. In our analysis of CMS data [3] we should take the sum of all B -mesons as it is was performed in the experiment.

5 Results

We apply PRA to describe $B\bar{B}$ -pair production data from CMS Collaboration at the CERN LHC [3]. The data were collected at the $\sqrt{S} = 7$ TeV. There are three samples of data which correspond to different values of leading jet transverse momentum in the event: $p_{TL} > 56$ GeV (A), $p_{TL} > 84$ GeV (B) and $p_{TL} > 120$ GeV (C). The leading jet is used to define the energy scale of the event and it is required to be within $|\eta(jet)| < 3.0$. This leading jet can be initiated either by b -quark or \bar{b} -quark production, which we describe by the LO hard subprocess (1), or by the hard gluon jet. We take into account the latter possibility by the NLO subprocess (3). For the jet reconstruction, the anti- k_T jet algorithm [28] with a distance parameter $R_{k_T} = 0.5$ was used. The visible kinematic range for the measurements was defined at the B -meson level by the requirements $|\eta(B, \bar{B})| < 2.0$ and $p_T(B) > 15$ GeV for both of the B -mesons. Originally, data consist sum of events with B -mesons and B -baryons, but we can ignore the small contribution from bottom baryons, which is about several percents of summed contribution.

The variables used for the characterization of the angular correlations between the two hadrons are the difference in azimuthal angles ($\Delta\phi$) and the difference in polar angles, usually expressed in terms of pseudorapidity ($\Delta\eta$), or the combined separation variable $\Delta R = \sqrt{\Delta\eta^2 + \Delta\phi^2}$.

In the PRA, the parton emission in hard subprocess and during evolution are not ordered in transverse momentum and we should use cuts on the transverse momenta of initial Reggeized gluons $\max(\sqrt{t_1}, \sqrt{t_2}) < p_{TL}$ to ensure, that the leading jet can be produced only in hard subprocess. After this, we consider LO contribution of subprocesses (1) requiring $\max(p_{Tb}, p_{T\bar{b}}) = p_{TL}$, and NLO subprocess (3) taking into account that $p_{Tg} = p_{TL}$ and with additional cut $\max(p_{Tb}, p_{T\bar{b}}) < p_{TL}$. If the ΔR distance between b and \bar{b} is smaller than R_{k_T} they are considered as one jet and we compare the sum of their transverse momenta with the threshold value of leading jet transverse momentum p_{TL} . It is important for calculation in region of first two bins, where $0 \leq \Delta\phi \leq 1$, $\Delta R \leq 0.5$.

Experimental uncertainties, related to the shape of $\Delta\phi$ and ΔR distributions are relatively small ($\sim 20-30\%$). They are indicated by the error-bars in the Fig. 3. However, an additional uncertainty in the absolute normalization of the cross-sections $\simeq \pm 47\%$ is reported in the Ref. [3]. It is not included into the error bars of the experimental points in the Fig. 3, as well as in the plots presented in the experimental paper. Taking this large uncertainty into account, it is reasonable to consider the overall normalization of the cross-section to be a free parameter, which is also the case in MC simulations presented in the Ref. [3]. Following this route we find, that to obtain a very good agreement of the central curve of our predictions both with the shape and normalization of all experimental spectra we have to multiply all our predictions by the universal factor $\simeq 0.4$. Since the major part of the reported normalization uncertainty is due to the uncertainty in the efficiency of identification of B -mesons, our finding seems to support the assumption, that the B -meson reconstruction efficiency is largely independent from the kinematics of the leading jet, and in particular, from the value of p_{TL} . In the plots below, we show theoretical predictions multiplied by the above-mentioned factor, however our default result is also compatible with experiment, if one takes into account full experimental uncertainties and the scale-uncertainty of our predictions.

In the Fig. 3 we present the comparison of the predictions of our model with $\Delta\phi$ and ΔR spectra from the Ref. [3]. Apart from the above-mentioned overall normalization uncertainty, our model does not contain any free parameters. In both LO (1) and NLO (3) contributions we set the renormalization and factorization scales to be equal to the p_T of the leading jet: $\mu_R = \mu_F = \xi p_{TL}$, where $\xi = 1$ for the central lines of our predictions, and we vary $1/2 < \xi < 2$ to estimate the scale-uncertainty of our prediction, which is shown in the following figures by the gray band. All numerical calculations has been performed using the adaptive MC integration routines from the CUBA library [29], mostly using the SUAVE algorithm, but with the cross-checks against the results obtained by VEGAS and DIVONNE routines.

We have obtained very good agreement between our predictions and experimental data both for $\Delta\phi$ and ΔR spectra at all values of p_{TL} . We have found that LO and NLO contributions are dominating in the different ranges of $\Delta\phi$ and ΔR . The LO contribution dominates at the large $\Delta\phi, \Delta R \geq 2$, but NLO contribution is extremely important for regions of small and moderate values of $\Delta\phi$ and ΔR .

6 Conclusions

We have calculated the angular spectra between beauty and anti-beauty mesons in proton-proton collisions in the LO approximation of the parton Reggeization approach consistently merged with the NLO corrections from the emission of additional hard gluon. We have obtained good agreement between our predictions and data from the CMS Collaboration at the energy $\sqrt{S} = 7$ TeV for $B\bar{B}$ angular correlations within uncertainties and without free parameters. The NLO contribution from the emission of additional real gluon for $B\bar{B}$ -pair production cross section in the k_T -factorization scheme has been calculated in the first time.

7 Acknowledgements

We are grateful to A. van Hameren for help in comparison between amplitudes obtained in the PRA and ones obtained using Monte-Carlo generator *Katie*.

This work was supported by the Ministry of Education and Science of Russia under Competitiveness Enhancement Program of Samara University for 2013-2020, project 3.5093.2017/8.9.

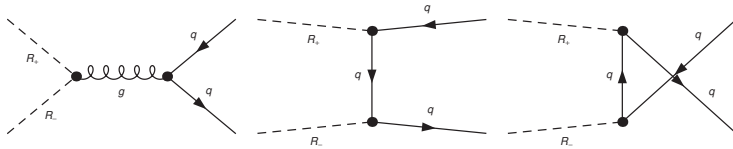


Figure 1. The Feynman diagrams of Lipatov's Effective Theory for the Reggeized amplitude of subprocess $R + R \rightarrow b + \bar{b}$.

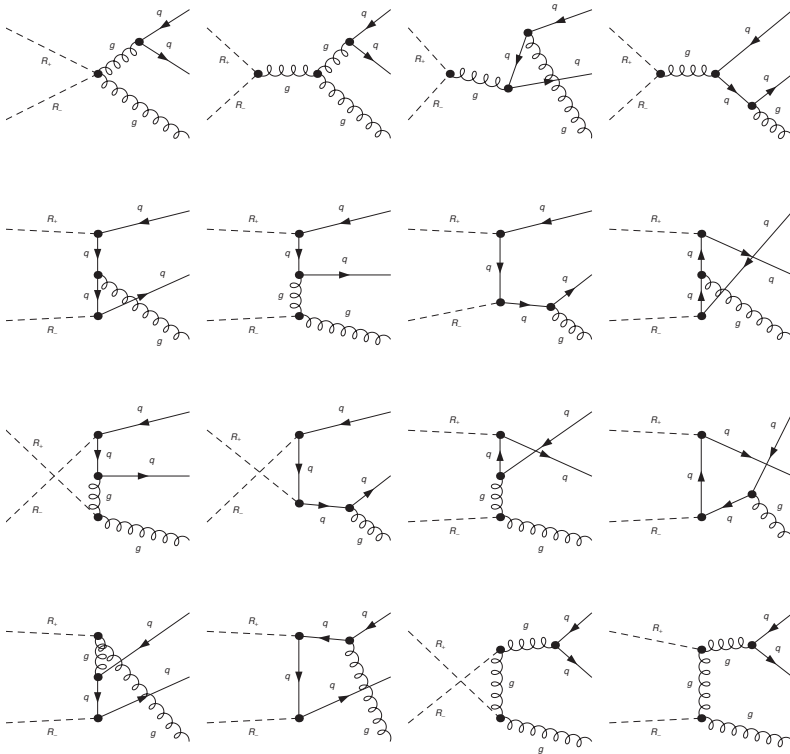


Figure 2. The Feynman diagrams of Lipatov's Effective Theory for the Reggeized amplitude of subprocess $R + R \rightarrow b + \bar{b} + g$.

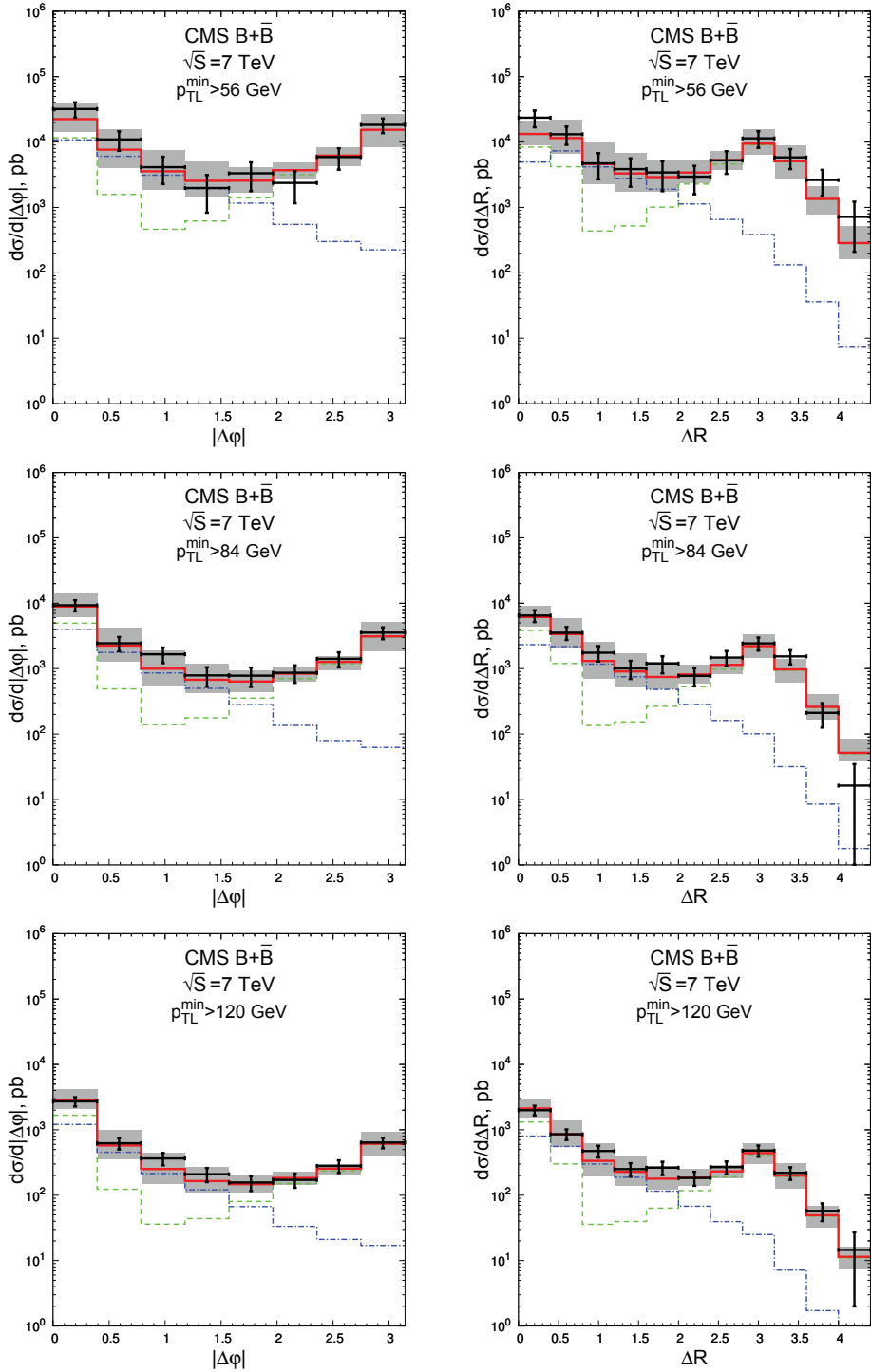


Figure 3. Comparison of the predictions for $\Delta\phi$ -spectra and ΔR -spectra of $B\bar{B}$ -pairs with the CMS data [3] at the different values of p_{TL} . Dashed line – contribution of the LO subprocess (1), dash-dotted line – contribution of the NLO subprocess (3), solid line – sum of LO and NLO contributions.

References

- [1] CDF Collaboration, T. Aaltonen et al., CDF note 8939, (2007).
- [2] ATLAS Collaboration, G. Aad et al., Eur. Phys. J. C **71**, 1846 (2011).
- [3] CMS Collaboration, JHEP **03**, 136 (2011).
- [4] M. A. Nefedov, V. A. Saleev, A. V. Shipilova, Phys. Rev. D **87**, 094030 (2013).
- [5] B. A. Kniehl, A. V. Shipilova, and V. A. Saleev, Phys. Rev. D **81**, 094010 (2010).
- [6] V. A. Saleev, A. V. Shipilova Phys. Rev. D **86**, 034032 (2012).
- [7] M. Nefedov and V. Saleev, Phys. Rev. D **92**, 094033 (2015).
- [8] R. Maciula, V. A. Saleev, A. V. Shipilova and A. Szczurek, Phys. Lett. B **758**, 458 (2016).
- [9] A. Karpishkov, V. Saleev and A. Shipilova, Phys. Rev. D **94**, 114012 (2016).
- [10] A. V. Karpishkov, M. A. Nefedov, V. A. Saleev and A. V. Shipilova, Int. J. Mod. Phys. A **30**, 1550023 (2015).
- [11] M. A. Kimber, A. D. Martin, and M. G. Ryskin, Phys. Rev. D **63**, 114027 (2001).
- [12] A. Karpishkov, M. Nefedov and V. Saleev, arXiv:1707.04068 [hep-ph], (2017).
- [13] A.D. Martin, et. al., Eur. Phys. J. C **63**, 189 (2009).
- [14] L. N. Lipatov, Nucl. Phys. B **452**, 369 (1995).
- [15] L. N. Lipatov and M. I. Vyazovsky, Nucl. Phys. B **597**, 399 (2001).
- [16] T. Hahn, Comput. Phys. Commun. **140**, 418 (2001).
- [17] M. Nefedov and V. Saleev, Phys. Rev. D **92**, 094033 (2015).
- [18] R. Mertig, M. Bohm, and A. Denner, Comput. Phys. Commun. **64**, 345 (1991).
- [19] T. Hahn and M. Perez-Victoria, Comput. Phys. Commun. **118**, 153 (1999).
- [20] A. van Hameren, arXiv:1611.00680 [hep-ph], (2016).
- [21] A. van Hameren and M. Serino, JHEP **07**, 010 (2015); K. Kutak, A. Hameren and M. Serino, JHEP **02**, 009 (2017).
- [22] A. van Hameren, J. High Energy Phys. **07**, 138 (2014).
- [23] B. A. Kniehl, G. Kramer, I. Schienbein, and H. Spiesberger, Phys. Rev. D **77**, 014011 (2008).
- [24] ALEPH Collaboration, A. Heister et al., Phys. Lett. B **512**, 30 (2001).
- [25] OPAL Collaboration, G. Abbiendi et al., Eur. Phys. J. C **29**, 463 (2003).
- [26] J. Binnewies, B. A. Kniehl, and G. Kramer, Phys. Rev. D **58**, 034016 (1998).
- [27] V. N. Gribov and L. N. Lipatov, Sov. J. Nucl. Phys. **15**, 438 (1972) [*Yad. Fiz.* **15**, 781 (1972)]; Yu. L. Dokshitzer, Sov. Phys. JETP **46**, 641 (1977) [*Zh. Eksp. Teor. Fiz.* **73**, 1216 (1977)]; G. Altarelli and G. Parisi, Nucl. Phys. **B126**, 298 (1977).
- [28] M. Cacciari, G.P. Salam and G. Soyez, JHEP **04**, 063 (2008).
- [29] T. Hahn, Comput. Phys. Commun. **168**, 78 (2005); J. Phys. Conf. Ser. **608**, 012066 (2015).